# Revisiting the Cobalt(II) hydration from Molecular Dynamics and X-ray Absorption Spectroscopy

Daniel Z. Caralampio[a] and Benjamin Reeves[b] and Maria R. Beccia[b] and José M. Martínez[a] and Rafael R. Pappalardo[a] and Christophe den Auwer[b] and Enrique Sánchez Marcos[a]

[a] Department of Physical Chemistry, University of Seville, 41012 Seville, Spain
[b] Université Côte d'Azur, Institut de Chimie de Nice, CNRS, UMR 7272, 06108 Nice, France

**ARTICLE HISTORY**
Compiled July 18, 2019

**ABSTRACT**

Solution chemistry of Co(II) is receiving a renewal attention due to the high interest for knowing the speciation in seawater of its $^{60}$Co radioactive isotope which appeared in the Japan sea as a consequence of the Fukushima-Daichii nuclear power plant accident. Experimental EXAFS and XANES spectra of a dilute Co(II) aqueous solutions have been recorded and structural data derived from their analysis. Based on QM calculations, an ab-initio intermolecular potential has been generated for the Co(II)–$H_2O$ interaction using the hydrated ion model that uses a polarizable and flexible solvent description through the MCDHO2 model. Classical molecular dynamics simulations of Co(II) in water have been performed and X-ray Absorption spectra have been simulated and compared with the experimental ones. Energetic, structural, dynamical and spectroscopical properties of the cobalt cation in solution have been computed and compared with previous experimental and theoretical data. These comparisons have assessed the good performance of the developed intermolecular potential.

**KEYWORDS**
Intermolecular potential and Polarizable and Flexible model and MCDHO2 potential and MD simulation and power spectrum

## 1. Introduction

The Fukushima-Daichii nuclear central accident, which happened in 2011, has stimulated the interest in different ion-containing aqueous solutions due to the speciation of some radioactive isotopes in the seawater surrounding the nuclear plant shores.[1, 2] The main challenge is to establish the physicochemical properties of these radioactive cations in aqueous media containing relatively high concentrations of marine salts. The latter are able to alter the behavior of radioactive material present in low concentration both, by electrostatic interactions, as supporting electrolytes, and by chemical bonding, as anion complexation.[3, 4] One of the involved radioactive cations is the $^{60}$Co that appears in its divalent oxidation state as a sub-product of the $^{127}$Cs decay.

The aim of this work is to establish a double experimental-theoretical reference of Co(II) in dilute aqueous solutions to be used in further studies of Co(II) solvated in the more complex seawater medium. To undertake this type of involved studies, it is convenient to establish reference data of simpler systems both at the XAS instrumental level and at the computer simulation level. This allows monitoring of the changes of physicochemical properties of the Co(II) from a dilute solution without other ions than its salt counterion to a seawater solution.

Table 1 collects a wide set of experimental and theoretical properties of Co(II) aqueous solutions which appeared in the literature. There is a general agreement about the Co(II) hexa-coordination at highly dilute aqueous solutions, because its octahedral aqua ion forms a stable high-spin $[Co(H_2O)_6]^{2+}$ ($d^7$) complex.[5] An infrared study together with a combined electronic spectroscopy and multi-reference quantum mechanical study support the six-fold

CONTACT E. Sánchez. Author. Email: sanchez@us.es

coordination as the most representative aqua ion structure in solution.[6, 7] X-ray diffraction studies[8, 9] proposed a first-shell Co-$O_I$ distance range of 2.00-2.10 Å and Levochkin et al.[9] a second hydration shell centered at 4.05 Å. EXAFS fittings found hexacoordination for the Co(II) aqua ion and a Co-$O_I$ range of 2.06-2.09 Å with Debye-Waller factors in the range 0.0038–0.0062 $Å^2$.[10–12] D'Angelo et al.[13], from the fitting of the XANES spectrum, proposed a hexahydrated ion with the Co-$O_I$ distance equals to 2.06 Å. This methodology was proposed originally by Benfatto and Della Longa.[14]

Several groups have performed computer simulations of Co(II)-containing aqueous solutions using classical and quantum mechanics Molecular Dynamics (MD) simulations.[12, 15, 16] There is a general agreement on the six-fold coordination of the first shell with a range of Co-$O_I$ distance of 2.07-2.27Å. For the second-shell hydration number, the range is 12-23 with Co-$O_{II}$ distances between 4.1 and 4.6 Å.

## 2. Methodology

### *2.1. $Co^{2+}$-$H_2O$ interaction potential building*

The exchangeable hydrated ion model[17, 18], a refinement of our original hydrated ion approach[19], allows the release of first-shell water molecules from the hydrated ions, i.e. water exchange is allowed. A flexible and polarizable $Co^{2+}$-$H_2O$ interaction potential has been built. Following the idea performed in a previous Scandium hydration study,[20] we have developed the cobalt-water intermolecular potential considering Co(II) hexahydrate structures, $[Co(H_2O)_6]^{2+}$, derived from the quantum-mechanical optimized structure. Distorted structures where Co-$H_2O$ distances and angles are changed according to the stretching and bending normal modes of the minimum energy octahedral structure were used to build the potential. As Co(II) transition metal cation is an open-shell system, the use of its hexahydrate instead of the bare cation to extract the quantum-mechanical interaction energies is particularly appropriate. The octahedral coordination complex formed by its aqua ion guarantees that its electronic state (quartet multiplicity)[16] is preserved along the geometrical deformations considered for the sampling, something that it would not have been preserved if bare $Co^{2+}$-$H_2O$ interactions were considered.

The QM calculations were carried out at the B3LYP level, using the ECP10MDF pseudopotential and the associated basis set of Stuttgart group for Co[21, 22] and the aug-cc-pVTZ basis set for O and H. To prospect the cobalt(II)-water potential energy surface, together with the $[Co(H_2O)_6]^{2+}$ minimum energy structure, the extraction of one water molecule from the $Co^{2+}$ aqua ion structure, a bending and the symmetric and assymmetric stretchings of the aqua ion were included in the intermolecular potential generation. Figure 1 displays some of the representative structure deformations used for the fitting. All calculation were performed with Gaussian 09.[23]

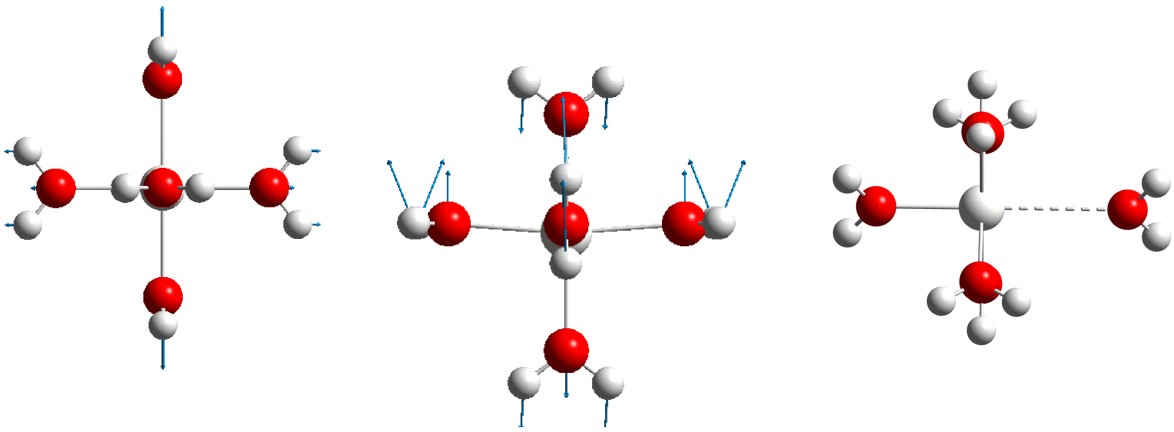

**Figure 1.** Representative set of deformations chosen from $Co^{2+}$ hexahydrate used to build the intermolecular potential. Arrows indicates the type of distortion (normal mode) considered in the hydrates. From left to right, asymmetric stretching mode, bending mode and shortening and lengthening of only one Co–$OH_2$ distance

The metal cation is defined as polarizable and the water molecules are defined by the MCDHO2 potential[24], a polarizable and flexible model, derived from the original mobile charge density harmonic oscillator model MCDHO.[25] Details about the potential employed

as well as the set of fitted coefficients for the new $Co^2$–$H_2O$ potential are collected in the Suplementary Material (SM). The obtained potential gives an accurate description of both energetic and structural properties of the mimimum energy hexahydrate: $E_{\rm int}$ = -342.7 kcal/mol (QM) vs. -342.5 kcal/mol (Pot) and a Co-$O_I$ distance of 2.110 Å (QM) vs. 2.113 Å (Pot). The whole set of structures considered in the fitting were 50 and the mean error of the fit was 1.5 kcal/mol.

## *2.2. Molecular dynamics simulations*

MD simulations in the canonical ensemble (NVT) at 300 K employing the Noose-Hoover thermostat with a relaxation time of 0.5 ps were carried out. A new modified version of the DL_POLY program (Classic version) [26] that incorporates the force field was employed. The polarizable character was described by means of the adiabatic shell model. The simulation box contained 1 $Co^{2+}$ cation and 1000 water molecules, with a box length of 31.098 Å in order to fit the experimental water density, 0.997 g/$cm^3$. Long-range interactions were treated by means of the Ewald sum. A trajectory with a 100 ps of equilibration time and 1 ns of production time was employed for the analysis.

## *2.3. Experimental XAS spectra*

Co K-edge XAS fluorescence spectra of a $CoCl_2$ 0.005M in HCl 0.05M aqueous solution were recorded in the MARS beamline at the SOLEIL Synchrotron Radiation source (Saclay, France). In this concentration range the stability of the aqua ion is high enough to prevent the formation of chloro-aquo complexes. This is confirmed by the vis-UV electronic spectrum of the sample, as well as by the EXAFS and XANES spectra which would had been highly modified if chloride ligands had replaced water molecules in the $Co^{2+}$ first coordination sphere. The change of EXAFS and XANES spectra of $Cr^{3+}$ aqua ion when chloride ligands replace water molecules in its first coordination shell has been shown in a previous study.[27] The storage ring operated at an energy of 2.5 GeV with a top electron current of 200 mA. The optics of the beamline essentially consist of a water-cooled double-crystal monochromator (FMB Oxford), which is used to select the incident energy of the X-ray beam and for horizontal focalization, and two large water-cooled reflecting mirrors (IRELEC/SESO) that are used for high-energy rejection (harmonic part) and vertical collimation and focalization. In this case, the monochromator was set with the Si(111) crystals. Energy calibration of the monochromator was done using Ni foil as reference at maximum first derivative equal to 8.333 keV. Because of the low concentration of the samples, EXAFS measurements were performed in fluorescence mode using a 13-element high purity germanium detector (ORTEC). The sample was kept in a specifically designed cell for diluted liquids (Ets CANAPLE) with kapton window. Three scans were carried out and the signal averaged.

EXAFS extraction was performed in $k^2\chi(k)$ with Athena code using a spline function.[28] Data adjustment was performed with Artemis code (Demeter version 0.9.25) in R space after Fourier transform between 2.4 and 12.5 Å-1.[28] Adjustment was performed with one shell of Co-O using the FEFF6 code[29] that is included in the Demeter version.

$k^2$-weigthed EXAFS spectrum and its Fourier Transform together with their fitting are plotted in Figure 2. XANES spectrum is plotted in Figure 7, it was recorded with an energy step of 0.5 eV in the edge.

## *2.4. Simulated XAS spectra*

Simulated Co K-edge EXAFS and XANES spectra have been computed using the FEFF 9.6 code [30]. They have been built by averaging the individual spectra of 500 evenly distributed snapshots. The Hedin-Lundqvist exchange-correlation potential was used to compute the electron density distribution within the SCF approach. The cutoff radius used to select the extension of the hydration water shell around the Co absorber atom was large enough to include well beyond the second hydration shell ($R_{\rm cut}$ = 8 Å, see RDF in Figure 3).

The $\Delta E_0$ applied for the simulated EXAFS spectrum was chosen such as it matches the first EXAFS oscillation at 3.5 $Å^{-1}$. Previous examples of the methodology applied to other highly-charged metal cations in water can be found elsewhere [17, 18, 31, 32]. A sphere of 6 Å around the cation was applied in the full multiple scattering formalism (FMS) for the XANES calculation.The same cutoff radius for selecting the extension of the hydration structure around the Co absorber atom than for EXAFS, *i.e.* 8 Å, was used. The SCF procedure provides a very good estimation of the edge position, thus the simulated spectrum has been shifted only -2.0 eV to overimpose the white line with the experimental one. FEFF input files for the EXAFS and XANES calculations are given in the SM.

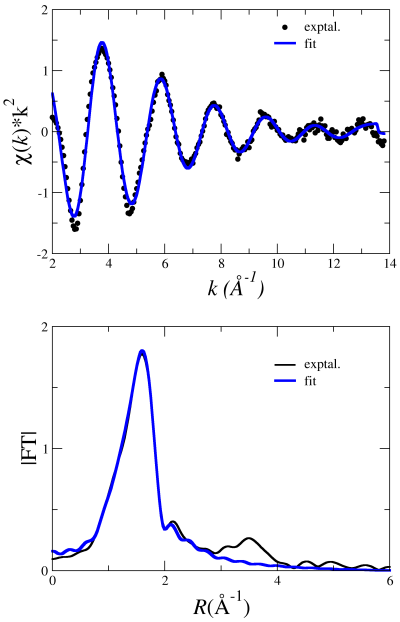


**Figure 2.** (a) Co K-edge $k^2$-weighted EXAFS spectrum (dotted line) and fit (blue line); (b) Modulus of Fourier Transform EXAFS spectrum (black line) and its fit (blue line). ($E_0 = 7727$ eV; inner correction potential, $\Delta E_0 = -2.9$ eV; amplitude reduction factor, $S_0^2 = 0.9$; $\chi^2_{red} = 4.74$; quality factor = 1.6%.)

## 3. Results and discussion

Figure 2 shows the experimental Co K-edge EXAFS spectrum (top Figure, dotted line) and its fit (top Figure, blue line), as well as the Fourier Transform of them (bottom Figure). The spectrum is a rather simple function with a good signal/noise ratio up to 13.5 $Å^{-1}$. The fit of the spectrum is obtained with the use of only a first-shell formed by 6 water molecules with a Co-O distance of 2.08 ± 0.01 Å and a Debye-Waller value (DW) of 0.0071 ± 0.0004 $Å^2$.

The Co-O and Co-H RDFs for $Co^{2+}$ in water obtained by the MD simulation are shown in Figure 3. The Co-O RDF (black line) has two well-defined peaks with maxima at 2.09 Å and 4.24 Å. The value for the Co-$O_I$ distance is similar to the value provided by the EXAFS fit, and within the range of values proposed in the literature. The Co-$O_{II}$ distance is shorter than the theoretical values previously proposed,[12, 15, 16] in the range 4.1-4.6 Å, but larger than the experimentally reported from X-ray diffraction measurements, 4.05 Å.[9] The depletion zone between the first and second peak indicates there are no water exchanges between these hydration shells during the simulation time. The running integration numbers are 6 and $\sim$ 15 for the first and second shell, respectively. Average tilt angle of the first-shell water molecules is 35°, what means that there is a significant trend to ion-dipole orientation, mediated by temperature effects and water interactions with second-shell water molecules. M-H RDF shows two maxima, one at 2.73 Å and the other at 4.87 Å, the integration of these peaks being $\sim$ 13.5 and $\sim$ 41.5.

First-shell DW computed as the average of the mean-square displacements of $R$(Co-$O_I$), $[\sigma_I^2 = < (R_I - \overline{R_I})^2 >]$, gives a value of 0.0082 $Å^2$, slightly higher than the value obtained from the EXAFS fit, and those experimental values previously reported, 0.0042-0.0062 $Å^2$.[10–12]

Another interesting structural parameter is the eccentricity index, $\varepsilon = < |\vec{R}_{M^{n+}} - \vec{R}_{CM}| >$,[33]. This index accounts for the assymmetry of the hydrated ion by calculating the average distance between the mass center of the first hydration shell and the central metal cation. For the $Co^{2+}$ hexahydrate, $\varepsilon = 0.11$ Å, a small value compared to what has been reported for other more labile ions, such as $Rb^+$ and $Cs^+$,[33] that reflects the robustness of this hydrated ion. The polarization of the closer water molecules by the cation presence is high in the first shell increasing their dipole moment by 0.7 D, whereas the increase in the second hydration shell is small, only 0.1 D (see Table 1).

An additional structural information to understand the hydration structure around $Co^{2+}$ is the hydrogen bond (HB) network formed by the successive hydration shells. Total average of HBs per first-shell water molecule is 2.15, being formed exclusively between first and second shell water molecules. 89% of these HBs are donated by the first-shell molecules to the second-shell molecules and the rest are HBs accepted by the first shell molecules. No HBs

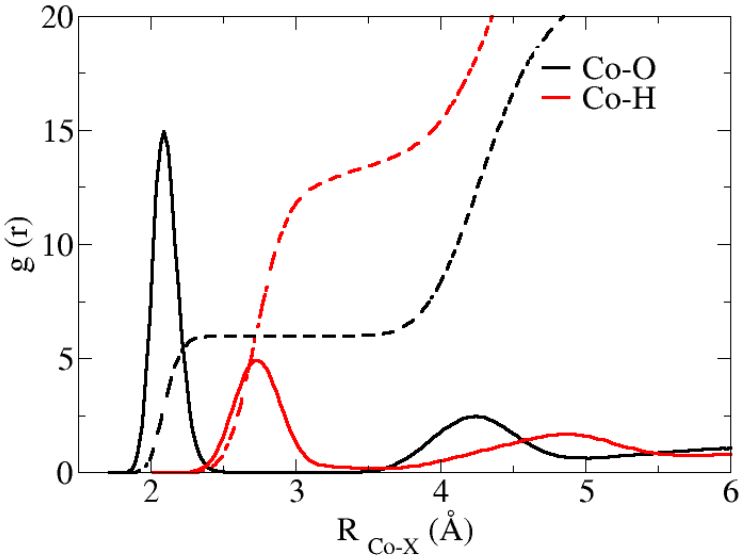


**Figure 3.** Radial distribution function Cobalt-Oxygen and Cobalt-Hydrogen.

among first-shell molecules are found. This can be understood on the basis of the average tilt angle, $\sim 34°$, that shows a marked ion-dipole orientation of the first shell water molecules, although fluctuations allow the occasional HB acceptor behavior of the first-shell water molecules(11%), and consequently more than two HBs per water molecule can be found.

Experimental mean residence time (MRT) values for first-shell water molecules are of $\sim$1 ms [34, 35]. These times are much longer than the simulation time, 1 ns, accordingly no water exchange was observed between first and second shell along the simulation. At this point it is worth noting that although the intermolecular potential built is based on the hydrated ion model, first-shell water molecules are treated as independent particles. This means that the water exchange is not prevented by any type of constraint but rather by the correct behavior of the employed potentials. The use of periodic boundary conditions causes an interparticle coupling with their neighboring images that reduces their motion and then their difusion coefficient. We have applied the Yeh and Hummer expression[36] to correct $D_0$ for a cubic cell. The corrected value obtained for $Co^{2+}$ is (0.6$\pm$ 0.1) $10^{-5}$ cm$^2$ s$^{-1}$, this value is similar to what was determined experimentally[37], $0.732\times10^{-5}$ cm$^2$ s$^{-1}$. This result on the $Co^{2+}$ dynamical behavior emphasizes the idea of the $Co^{2+}$ aqua ion as the species responsible of the ion mobility, since MRTs guarantees that the ion and its first hydration shell define the dynamic entity describing the correct diffusional behavior in solution.

From the energetic point of view, the hydration enthalpy obtained in this work, -479 kcal/mol, agrees fairly well with the experimental data, -487 kcal/mol.[37]

Water reorientational times for the first and second order correlation functions associated to the motion of the dipole moment vector $\mu$, the hydrogen-hydrogen vector HH, the normal vector to the molecular plane $\perp$ and the oxygen-hydrogen axis OH have been computed. Reorientational times ($\tau_1$ and $\tau_2$) have been calculated from the correlation functions defined in equations 1 and 2

$$C_{1,i}(t) = \left\langle \vec{u}_i(0)\vec{u}_i(t) \right\rangle \tag{1}$$

$$C_{2,i}(t) = \frac{1}{2}\left\langle 3(\vec{u}_i(0)\vec{u}_i(t))^2 - 1 \right\rangle \tag{2}$$

$\vec{u}_i$ is the unit vector representing any of the reference directions previously mentioned. The re-orientational correlation functions were calculated from a 1 ns simulation with a 0.01 ps time interval between structures. Re-orientational times of the first shell water molecules are shown in Table 2. Values for the MCDHO2 water molecule are also included. The relative re-orientational times $\tau_{1,n,first-shell}/\tau_{1,n,bulk}$ of this work are close to the relative values obtained by Rode and col. in their QM/MM simulation. [15] The mobility restriction suffered

**Table 1.** Properties of $Co^{2+}$ aqueous solution. Standard deviation in parenthesis.

| Property | this work EXAFS | this work MD | Literature |
|---|---|---|---|
| $R_{\text{M-O}_\text{I}}$ (Å) | 2.08 | 2.09 | 2.0[9], 2.10[8], 2.092[12] 2.097[11], 2.07-2.14[16], 2.08[10, 38] 2.06[13], 2.17-2.27[15] |
| $CN_\text{I}$ | 6.0 | 6.0 | 6.0[9, 10, 12, 13, 16], 6.0-5.3[8], 6.7[11] 6.5[6] |
| DW (Å$^2$) | 0.0071 | 0.0082 | 0.012-0.015[16], 0.0038-0.0062[12], 0.0065[11] |
| tilt angle$_\text{I}$ (°) | | 34(4) | 18[15] |
| $\varepsilon$ (Å) | | 0.11 | |
| $R_{\text{M-O}_\text{II}}$ (Å) | | 4.24 | 4.05[9], 4.40[12], 4.10-4.28[16] 4.6[15] |
| $CN_\text{II}$ | | 15.0 | 8[9], 12.7[12], 12.48-13.18[16] 15.9-22.7[15] |
| tilt angle$_\text{II}$ (°) | | 64(4) | 37[38] |
| $\Delta\mu_\text{I}$ (D) | | 0.7(0.3) | |
| $\Delta\mu_\text{II}$ (D) | | 0.1(0.3) | |
| MRT($t^*=0$) (ps) | | $\infty$ | $\infty$[38], $\sim 1\times10^6$[35] |
| MRT($t^*=2$) (ps) | | $\infty$ | |
| $\Delta H_\text{hyd}$ (kcal/mol) | | –479(18) | –487[37] |
| $D_\text{o}$ ($10^{-5}$ cm$^2$/s) | | 0.6(0.1) | 0.732[37] |

by first-shell water molecules with respect to a bulk water molecule is clearly observed in both first- and second-order re-orientational times whose values for first-shell molecules are roughly three times longer than for those of bulk. However, in the case of $\tau_{i,\mu}$, i.e. $C_2$ molecular axis, the ratio becomes higher than ten times. This shows how first-shell water molecules hardly modify the ion-dipole orientation.

**Table 2.** First, $\tau_{1,n}$, and second order, $\tau_{2,n}$, re-orientational times of first shell water molecules with respect to the main rotational water axis ($\mu$, dipole moment; HH direction, $\perp$, normal to molecular plane; OH direction

| | $\tau$ (ps) | | | | | | | |
|---|---|---|---|---|---|---|---|---|
| Water Molecule | $\tau_{1,\mu}$ | $\tau_{2,\mu}$ | $\tau_{1,\text{HH}}$ | $\tau_{2,\text{HH}}$ | $\tau_{1,\perp}$ | $\tau_{2,\perp}$ | $\tau_{1,\text{OH}}$ | $\tau_{2,\text{OH}}$ |
| 1st. shell | 74 | 25 | 16 | 10 | 12 | 4 | 23 | 8 |
| Bulk | 5 | 2 | 6 | 3 | 4 | 2 | 6 | 3 |

The power spectra of the $Co^{2+}$ aqua ion have been computed by means of the Fourier Transform of the velocity autocorrelation functions (FT-VAC) of cobalt and first-shell oxygen atoms derived from MD simulation. Figure 4 shows the power spectra of the aqua ion isolated, i.e. in gas phase, (top figure) and in aqueous solution (bottom figure). The hexahydrate power spectrum in gas phase presents two peaks at low frequency, 105 and 160 cm$^{-1}$, associated to intermolecular bending modes, whereas at higher frequencies two bands, which can be associated to the Co-O stretching normal mode region, appear at ∼300 and 420 cm$^{-1}$. Analysis of dynamical variables associated to internal coordinates combination indicates that the peak at $\sim$ 300 cm$^{-1}$ corresponds to the $E_{2\text{g}}$ mode, and the symmetric breathing $A_\text{g}$ mode corresponds to the band centered at 420 cm$^{-1}$. The power spectrum in solution shows how the inclusion of second-shell interactions with the aqua ion widens the sharp gas-phase peaks. These solvent effects induce slight red-shifts of the bands leading to a symmetric stretching normal modes at $\sim$ 390 cm$^{-1}$, value close to the experimental value derived from Raman measurements by Kano, $\sim$ 380 cm$^{-1}$.[39]

Figure 5 shows the Co $K$-edge $k^2$-weigthed EXAFS spectrum corresponding to the experimental measurement of the very dilute $CoCl_2$ aqueous solution and the simulated EXAFS spectrum derived from evenly-spaced snapshots taken from the $Co^{2+}$ MD simulation (red line). This simulated spectrum was calculated including all atoms, i.e. cobalt, oxygen and

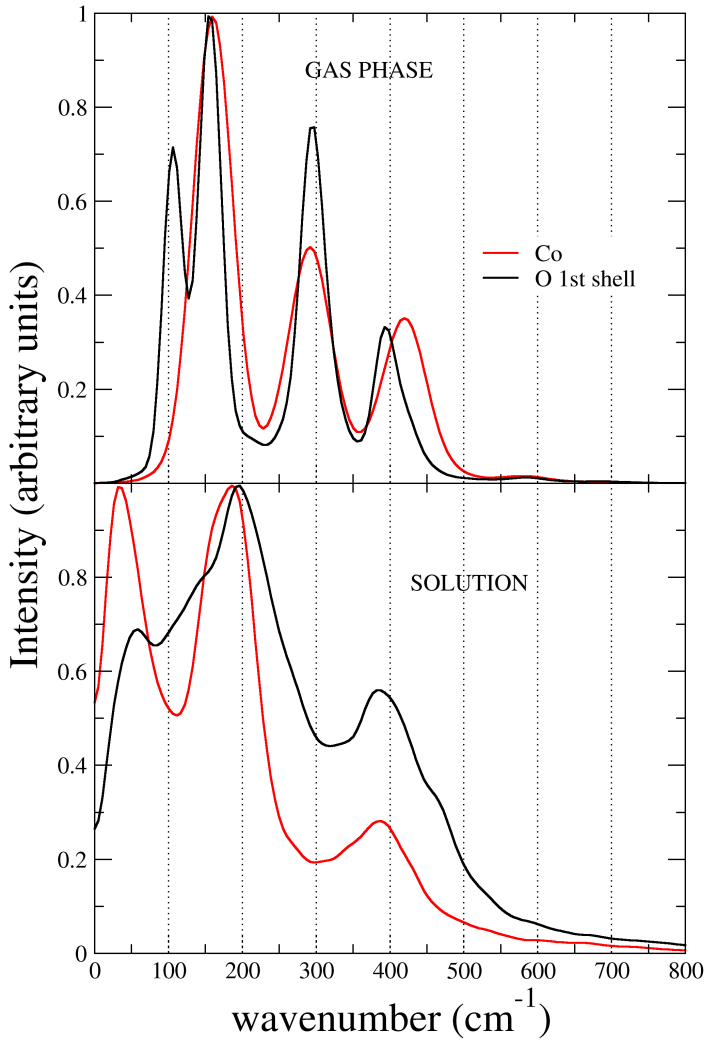


**Figure 4.** Power spectra of the cation (red line) and oxygen atoms of the $Co^{2+}$ aqua ion (black line) in gas phase (top) and in solution (bottom).

hydrogen, in the SCF calculation of backscattering potentials and in the scattering phenomena, using a $R_{\mathrm{cutoff}} = 8$ Å for the snapshots. This criterium guarantees that all contributions of the second hydration shell to the scattering were included in the EXAFS. It is observed a general good agreement in the frequency and the intensity of the signal up to 13.5 $\mathrm{Å}^{-1}$. Bearing in mind that the developed potential is based on quantum-mechanical calculations, the ensemble of structures contributing are completely independent of empirical information. This agreement gives confidence in the structural information derived from the intermolecular potential developed.

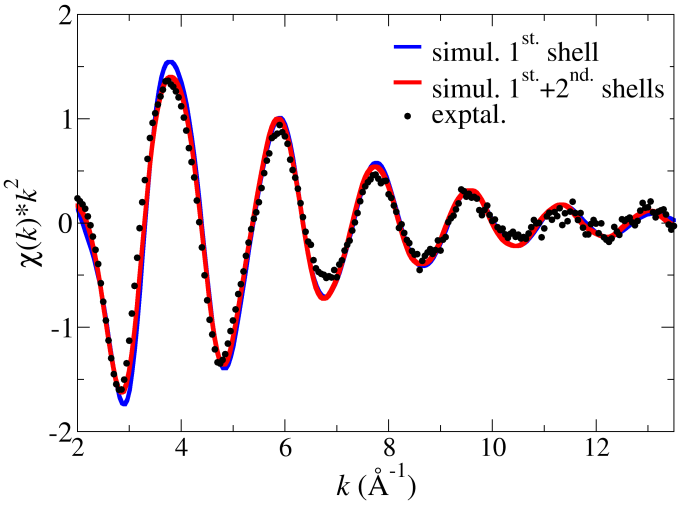


**Figure 5.** $k^2$-weighted Co $K$-edge EXAFS spectra of $Co^{2+}$ in aqueous solution: experimental spectrum (black dots) and simulated spectra including the first hydration shell (blue line) or the first and second hydration shells (red line).

The good experimental-theoretical agreement allows us to revisit in this well-defined sample the role of the second shell water molecules and the hydrogen atoms acting as backscatterers. There are previous studies of ions in solution where the simulated EXAFS spectrum considered the inclusion of hydrogen atoms in the calculation,[12] whereas in others it was considered that its inclusion exagerated the EXAFS signal intensity[40–42]. It has also been discussed about the capabilities of the EXAFS technique to characterize the second hydration shell.[12, 31, 41, 43, 44].

To study the role of the second hydration shell, we have computed the simulated spectrum including only the first hydration shell atoms in the calculation, a $R_{\mathrm{cutoff}} = 3$ Å was applied to the snapshots, then only the $[Co(H_2O)_6]^{2+}$ structure was accounted for computing the spectrum (see blue line in Figure 5 ). There is a slight difference, with respect to the spectrum simulated with two shells, in intensity at low $k$ values (2.5-4 $\mathrm{Å}^{-1}$) but at higher $k$ the spectra overlap. This subtle difference indicates that for a divalent aqua ion such as that of $Co^{2+}$ it is not possible to extract information about the second hydration shell, differing from what has been concluded in the case of stable and light trivalent transition metal cations.[31, 43, 45]

To check hydrogen effects on the EXAFS signal we have computed the spectrum excluding the scattering paths involving hydrogen atoms (green line in Figure 6). The comparison with the whole simulated spectrum (red line in Figure 6) shows that both spectra almost overimpose . This indicates that the new formalism of FEFF9.6 code[30, 46] has improved the description of hydrogen backscattering contribution.

Analysis of XANES spectrum becomes an additional and complementary information to that derived from EXAFS, particularly when it is possible to combine it with microscopic data obtained from an external source to the XAS technique, i.e. computer simulations based on statistical methods. Evenmore, a minimization procedure has been proposed to find a structure that reproduces the experimental XANES spectrum.[14]

Figure 7 shows the comparison between the Co K-edge experimental XANES recorded in this study and the simulated spectra derived from the snapshot set taken from the 1 ns MD simulation. The FEFF9.6 code was used for the computation of the XANES spectrum of each individual snapshot, considering the two already used $R_{\mathrm{cutoff}}$ values for the EXAFS computations (8 Å and 3 Å). It is worth pointing out that we are not trying to simulate the pre-edge $1s \rightarrow 3d$ forbidden transition. Because of the SCF nature of FEFF computations, the simulated spectra have been only shifted by $\sim$ -5 eV in order to overimpose the absolute position of the computed Co $K$-edge. It is remarkable the reproduction of the experimental XANES spectrum by the simulated ones in several items: the intensity of the white line and

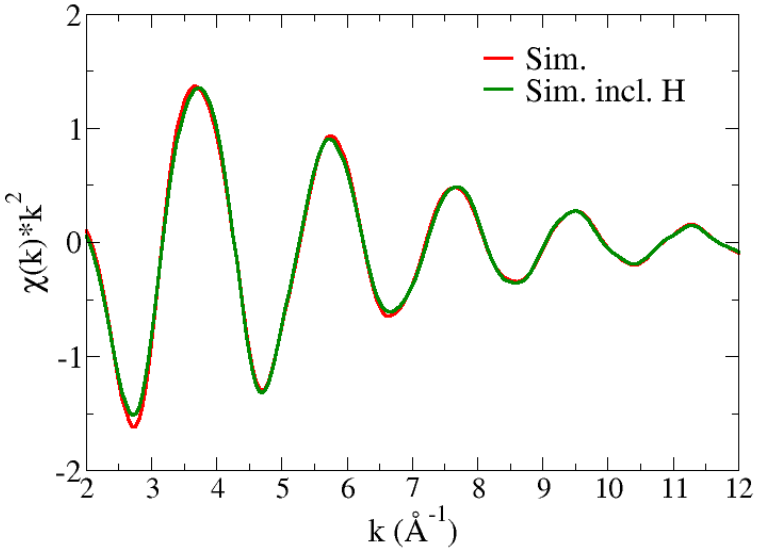


**Figure 6.** $k^2$-weighted Co $K$-edge simulated EXAFS spectra of $Co^{2+}$ in aqueous solution: including (green line) or excluding (red line) hydrogen atoms as backscaterers in the computation.

the second resonance, the coherent positions of their respective peaks and the presence of a small hump in between these two maxima. According to Natoli's rule[47], where the energy gap between the white line and its second resonance is related to the absorber-backscaterer distance, we must conclude that the Co-$O_I$ distance provided by the MD simulation is strongly supported by independent experiments.

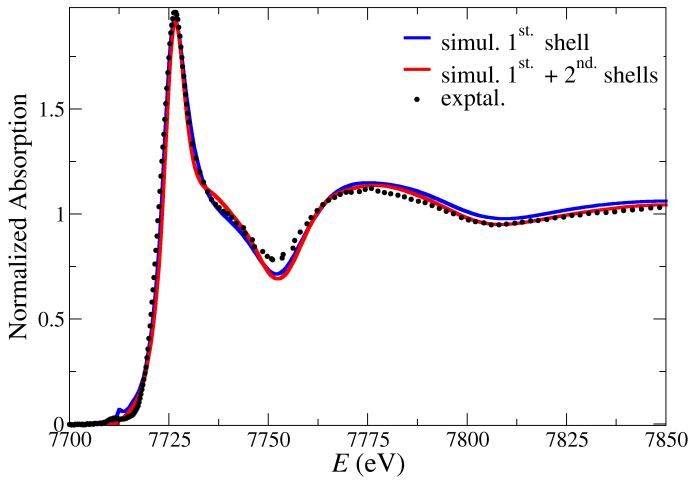


**Figure 7.** $K$-edge XANES spectra of a $Co^{2+}$ aqueous solution, experimental spectrum (black dots) and simulated spectrum with the first hydration shell (blue line) or the first and second hydration shells (red line).

A second interesting XANES feature is the small hump at $\sim$ 7737 eV. Figure 7 only shows slight differences between the spectrum considering one hydration shell (blue line) and that using two hydration shells (red line). The hump after the white line seems to be better reproduced by the one-shell spectrum, conversely the region above 7760 eV is better reproduced by the two-shell spectrum. In previous studies on some trivalent cations we had assigned this post-edge feature to the presence of a robust second hydration shell[31, 32, 48], as well as D'Angelo et al. assigned it in the case of $Ni^{2+}$.[49] One can observe that the

inclusion of the second hydration shell mainly changes the hump region rising this feature, although a change of slope is already present when the computation only includes the first hydration shell. This suggests that the possibility of extracting second hydration shell structural information from XANES is a difficult matter. This information could be only extracted if a well-tempered experimental-theoretical synergy was applied.

## 4. Concluding Remarks

$Co^{2+}$-containing dilute aqueous solution has been studied from both experimental and theoretical techniques. On one side, Co *K*-edge EXAFS and XANES spectra have been recorded and analyzed by standard fitting procedure as well as by combining them with theoretical results derived from classical MD simulations. A new intermolecular potential to describe $Co^{2+}$–$H_2O$ interaction based on the exchangeable hydrated ion model has been developed. The potential was built taking as reference quantum-mechanical interaction energies. The potential performance has been tested against experimental and theoretical results, showing a fair description of energetic, structural, dynamical and spectroscopical properties. In addition to the well known hexacoordination of its first-shell, a Co-$O_I$ distance of 2.08±0.01 or 2.09±0.01Å is proposed depending on EXAFS fitting or MD simulation, respectively. From MD simulations, Co-O RDF shows a well-defined second peak corresponding to a second hydration shell composed by $\sim$ 15 water molecules centered at 4.24 Å. The fair agreement between the experimental EXAFS and XANES spectra with those simulated from the statistical average of a large number of MD snapshots leads to get strong confidence in the previous structural data. The use of cuttoff radii in the snapshots used for the simulated XAS spectra allows us to test the impact of the second hydration shell on EXAFS and XANES features. It is shown that for this divalent transition metal cation aqueous solution, in both the EXAFS and XANES cases this effect is almost negligeable, suggesting that the experimental detection of the second hydration shell could hardly be achieved. Further studies based on this well-tested intermolecular potential will be used as reference in the simulation of Co(II) salts in the presence of seawater as well as for the analysis of future experimental XAS spectra of the similar kind of solutions.

## 5. Acknowledgements

DZC thanks to Junta de Andalucia of a postdoctoral fellowship (proyecto de excelencia P11-FQM7607). We thank the synchrotron radiation source of SOLEIL (France) for supplying us beamtime at MARS beamline (experimental number 20160305) and Dr. P.L. Solari for the technical support during XAS measurements. We thank the Spanish Ministerio de Ciencia, Innovación y Universidades for financial support (PGC2018-099366-B-I00).

## References

[1] Y.H. Koo, Y.S. Yang and K.W. Song, Prog. Nucl. Ener. **74**, 61 (2014).
[2] K. Hain, T. Faestermann, N. Famulok, L. Fimiani, J. Gómez-Guzmán, G. Korschinek, F. Kortmann, C. Lierse v. Gostomski, P. Ludwig and T. Shinonaga, Nucl. Instrum. Methods Phys. Res. B **361**, 505 (2015).
[3] J. Barthel, H. Krienke and W. Kunz, *Physical Chemistry of Electrolyte Solutions* (Steinkopff, Darmstadt, 1998).
[4] M. Maloubier, P.L. Solari, P. Moisy, M. Monfort, C. den Auwer and C. Moulin, Dalton Trans. **44**, 5417–5427 (2015).
[5] R. Akesson, L. Pettersson, M. Sandström and U. Wahlgren, J. Am. Chem. Soc. **116**, 8691–8704 (1994).
[6] P. Bergström and J. Lindgren, Inorg. Chem. **31** (8) (1992).
[7] H. Gilson and M. Krauss, J. Phys. Chem. A **102**, 6525–6532 (1998).
[8] H. Ohtaki and T. Radnai, Chem. Rev. **83**, 1157–1204 (1993).
[9] S.F. Levochkin, P.R. Smirnov and V.N. Trostin, Zh. Strukt. Khim. **75** (8), 1246–1251 (2004).
[10] Y. Inada, H. Hayashi, K. Sugimoto and S. Funahashi, J. Phys. Chem. A **103**, 1401–1406 (1999).
[11] C. Chen and K. Hayes, Geochim. Cosmochim. Acta **63** (19/20), 3205–3215 (1999).
[12] P. D'Angelo, V. Barone, G. Chillemi, N. Sanna, W. Meyer-Klauche and N.V. Pavel, J. Am. Chem. Soc. **124**, 1958–1967 (2002).

[13] P. D'Angelo, M. Benfatto, S.D. Longa and N. Pavel, Phys. Rev. B **66**, 064209(1–7) (2002).
[14] M. Benfatto and S. Della Longa, J. Synchrotron Rad. **8**, 1087–1094 (2001).
[15] R. Armunanto, C. Schwenk, A. Bambang and B. Rode, Chem. Phys. **295**, 63–70 (2003).
[16] R. Spezia, M. Duvail, P. Vitorge, T. Cartailler, J. Tortajada, G. Chillemi and P. D'Angelo, J. Phys. Chem. A **110**, 1381–13088 (2006).
[17] E. Galbis, J. Hernández-Cobos, C. den Auwer, C.L. Naour, D. Guillaumont, E. Simoni, R.R. Pappalardo and E. Sánchez Marcos, Angew. Chem. Int. Ed. **22**, 3811–3815 (2010).
[18] E. Galbis, J. Hernández-Cobos, R.R. Pappalardo and E. Sánchez Marcos, J. Chem. Phys. **140**, 214104(1–11) (2014).
[19] J.M. Martínez, R.R. Pappalardo and E. Sánchez Marcos, J. Am. Chem. Soc. **121**, 3175–3184 (1999).
[20] D.Z. Caralampio, J.M. Martínez, R.R. Pappalardo and E. Sánchez Marcos, Theor. Chem. Acc. **136** (4), 47(1–8) (2017).
[21] M. Dolg, U. Wedig, H. Stoll and H. Preuss, J. Phys. Chem. **86** (866), 1998 (1998).
[22] J.M.L. Martin and A. Sundermann, J. Chem. Phys. **114**, 3408 (2001).
[23] M.J. Frisch, G.W. Trucks, H.B. Schlegel, G.E. Scuseria, M.A. Robb, J.R. Cheeseman, G. Scalmani, V. Barone, B. Mennucci, G.A. Petersson, H. Nakatsuji, M. Caricato, X. Li, H.P. Hratchian, A.F. Izmaylov, J. Bloino, G. Zheng, J.L. Sonnenberg, M. Hada, M. Ehara, K. Toyota, R. Fukuda, J. Hasegawa, M. Ishida, T. Nakajima, Y. Honda, O. Kitao, H. Nakai, T. Vreven, J.A. Montgomery, Jr., J.E. Peralta, F. Ogliaro, M. Bearpark, J.J. Heyd, E. Brothers, K.N. Kudin, V.N. Staroverov, R. Kobayashi, J. Normand, K. Raghavachari, A. Rendell, J.C. Burant, S.S. Iyengar, J. Tomasi, M. Cossi, N. Rega, J.M. Millam, M. Klene, J.E. Knox, J.B. Cross, V. Bakken, C. Adamo, J. Jaramillo, R. Gomperts, R.E. Stratmann, O. Yazyev, A.J. Austin, R. Cammi, C. Pomelli, J.W. Ochterski, R.L. Martin, K. Morokuma, V.G. Zakrzewski, G.A. Voth, P. Salvador, J.J. Dannenberg, S. Dapprich, A.D. Daniels, O. Farkas, J.B. Foresman, J.V. Ortiz, J. Cioslowski and D.J. Fox, *Gaussian 09 Revision D.01* Gaussian Inc. Wallingford CT, 2009.
[24] A. Villa, B. Hess and H. Saint-Martin, J. Phys. Chem. B **113**, 7270–7281 (2009).
[25] H. Saint-Martin, J. Hernández-Cobos, M.I. Bernal-Uruchurtu, I. Ortega-Blake and H.J.C. Berendsen, J. Chem. Phys. **113**, 10899–10912 (2000).
[26] W. Smith, T. Forester and I.T. Todorov, *The DL_POLY Classic* STFC Daresbury Laboratory, Daresbury, 2012.
[27] S. Díaz-Moreno, A. Muñoz-Páez, J.M. Martínez, R.R. Pappalardo and E. Sánchez Marcos, J. Am. Chem. Soc. **118**, 12654–12664 (1996).
[28] B. Ravel and M. Newville, J. Synchrotron Rad. **12**, 537–541 (2005).
[29] S. Zabinsky, J. Rehr, A. Ankudinov, R. Albers and M. Eller, Phys. Rev. B **52**, 2995–3009 (1995).
[30] J.J. Rehr, J.J. Kas, F.D. Vila, M.P. Prange and K. Jorissen, Phys. Chem. Chem. Phys. **12**, 5503–5513 (2010).
[31] P.J. Merkling, A. Muñoz-Páez and E. Sánchez Marcos, J. Am. Chem. Soc. **124**, 10911–10920 (2002).
[32] F. Carrera, F. Torrico, D.T. Richens, A. Muñoz-Páez, J.M. Martínez, R.R. Pappalardo and E. Sánchez Marcos, J. Phys. Chem. B **111**, 8223–8233 (2007).
[33] D.Z. Caralampio, J.M. Martínez, R.R. Pappalardo and E. Sánchez Marcos, Phys. Chem. Chem. Phys. **19**, 28993–29004 (2017).
[34] L. Helm and A. Merbach, Coord. Chem. Rev. **187**, 151–181 (1999).
[35] D.T. Richens, *The Chemistry of Aqua Ions* (John Wiley, Chichester, 1997).
[36] I.C. Yeh and G. Hummer, J. Phys. Chem. B **108**, 15873–15879 (2004).
[37] Y. Marcus, *Ions in solution and their solvation.* (John Wiley & Sons, New York, 2015).
[38] G. Chilemi, P. D'Angelo, N.V. Pavel, N. Sanna and V. Barone, J. Am. Chem. Soc. **124** (9), 1968–1976 (2002).
[39] H. Kanno, J. Phys. Chem. **92**, 4232–4236 (1988).
[40] B.J. Palmer, D.M. Pfund and J.L. Fulton, J. Phys. Chem. **100**, 13393–13398 (1996).
[41] L. Campbell, J. Rehr, G. Schenter, M. McCarthy and D. Dixon, J. Synchrotron. Rad. **6**, 310–312 (1999).
[42] F. Jalilehvand, D. Spangberg, P. Lindqvist-Reis, K. Hermansson, I. Persson and M. Sandström, J. Am. Chem. Soc. **123**, 431–441 (2001).
[43] H. Sakane, A. Muñoz-Páez, S. Díaz-Moreno, J.M. Martínez, R.R. Pappalardo and E. Sánchez Marcos, J. Am. Chem. Soc. **120**, 10397–10401 (1998).
[44] P.J. Merkling, A. Muñoz-Páez, J.M. Martínez, R.R. Pappalardo and E. Sánchez Marcos, Phys. Rev. B **64**, 012201 (2001).
[45] A. Muñoz-Páez, R.R. Pappalardo and E. Sánchez Marcos, J. Am. Chem. Soc. **117**, 11710–11720

(1995).
[46] J.J. Rehr, J.J. Kas, M.P. Prange, A.P. Sorini, Y. Takimoto and F.D. Vila, C. R. Physique **10**, 548–559 (2009).
[47] A. Bianconi, M. Dell'Ariccia, A. Gargano and C.R. Natoli, in *Springer Series in Chemical Physics*, edited by A. Bianconi, A. Incoccia and S. Stipcich (Springer-Verlag, Berlin, 1983), Vol. 27, pp. 57–61.
[48] P.J. Merkling, A.Muñoz-Páez, R. Pappalardo and E. Sánchez Marcos, Phys. Rev. B **64**, 092201 (2001).
[49] P. D'Angelo, O.M. Roscioni, G. Chillemi, S. Della Longa and M. Benfatto, J. Am. Chem. Soc. **128**, 1853–1858 (2006).